buildings

MDPI

Article

Research on the Spatial Structure of the Beijing–Tianjin–Hebei Urban Agglomeration Based on POI and Impervious Surface Coverage

Tiange Zhang, Xia Zhu *, Yuanping Liu, Cui Jia and Huimin Bai

School of Remote Sensing and Information Engineering, North China Institute of Aerospace Engineering, Langfang 065000, China; ztg@stumail.nciae.edu.cn (T.Z.); liuyuanping@nciae.edu.cn (Y.L.); jiacui@nciae.edu.cn (C.J.); hm_bai@stumail.nciae.edu.cn (H.B.)
* Correspondence: zhuxia1201@nciae.edu.cn

Abstract: Exploring urban spatial structures through spatial coupling analysis methods is an important method to provide theoretical support for the construction of sustainable urban structures. In order to make up for the neglect of POI species differences in previous studies, information entropy was introduced to calculate POI confusion, and a comprehensive POI index was constructed by combining kernel density and the entropy weight method; impervious surface coverage was extracted based on land cover data. The spatial distribution of the Beijing–Tianjin–Hebei urban agglomeration and some typical cities was analyzed by coupling two types of data using the dual-factor mapping method. The research indicates the following: (1). The spatial distribution of the two sets of data in the Beijing–Tianjin–Hebei region is highly consistent, indicating a state of high spatial coupling; Beijing has the highest proportion of coupling in the same region at the city level (73.39%). (2). The areas with different coupling of the two types of data are mainly distributed in the urban fringe areas transitioning from the city center to the suburbs, as well as in large-scale areas with single functionality such as airports, scenic spots, and ports. This study shows that analysis combining the POI comprehensive index and impervious surface coverage can effectively characterize urban spatial structure characteristics, providing a new perspective for the study of the spatial structure of the Beijing–Tianjin–Hebei urban agglomeration. It is of great significance for a deeper understanding of the laws of urban agglomeration spatial structures and guiding the coordinated development of the Beijing–Tianjin–Hebei urban agglomeration.

Keywords: urban spatial structure; POI; impervious surface coverage; coupling analysis; Beijing–Tianjin–Hebei

check for updates

Citation: Zhang, T.; Zhu, X.; Liu, Y.; Jia, C.; Bai, H. Research on the Spatial Structure of the Beijing–Tianjin–Hebei Urban Agglomeration Based on POI and Impervious Surface Coverage. *Buildings* **2024**, *14*, 1793. https://doi.org/10.3390/buildings14061793

Academic Editor: Haifeng Liao

Received: 6 May 2024
Revised: 4 June 2024
Accepted: 5 June 2024
Published: 13 June 2024

Copyright: © 2024 by the authors. Licensee MDPI, Basel, Switzerland. This article is an open access article distributed under the terms and conditions of the Creative Commons Attribution (CC BY) license (https://creativecommons.org/licenses/by/4.0/).

1. Introduction

The acceleration of urbanization processes has profound implications for peri-urban regions, as the expansion of urban construction areas and the surge in human social activities have led to significant changes in urban spatial structures [1]. Built-up areas generally refer to urbanized regions with complete basic infrastructure and public facilities, developed extensively within the urban administrative boundaries [2]. Since the reform and opening-up, China's urbanization growth rate has been among the highest globally, with the urban built-up area expanding from 7000 square kilometers in 1981 to 60,700 square kilometers in 2020 [3]. In recent decades, the rapid expansion of urbanization has become an unstoppable trend in modern society, transcending a mere economic and social phenomenon to evolve into a complex ecological and environmental dilemma [4]. The disorderly expansion of construction land encroaches upon cultivated land, grassland, and forest land. The increase in residential space composed of construction land impedes the development of ecological space, complicating spatial planning and intensifying regional spatial conflicts [5]. This scenario raises the requirements for urban planning and management. Currently, China is experiencing rapid economic

growth, accelerating urbanization, the formation of urban built-up areas, and a swift expansion of the urban scale [6]. Obtaining the form of urban built-up areas efficiently and accurately and studying the change trend of urban scales have become the hotspots and key contents of urban spatial structure research [7]. This can not only rationally lay out urban space to promote urban development [8] but also guide the adjustment of urban spatial density planning [9] and avoid resource shortage or waste caused by the imbalance of urban building or functional area density [10].

In the relevant research on urban spatial planning, impervious surface data are indispensable and important data in the study of urban built-up areas [11]. These data can effectively represent urban physical spatial characteristics, especially the distribution of buildings, roads, and other infrastructure, and are an important indicator to measure the level of urbanization development and the ecological environment status. They provide essential foundational data support for research on urban spatial structures [12]. Numerous studies have utilized impervious surface data to explore urban development processes and conduct spatiotemporal dynamic analyses [13–15]. For instance, Zhou [16] introduced impervious surface coverage and landscape fragmentation as primary indicators for distinguishing urban fringe areas, with population density as a supplementary indicator, to construct an identification index system for urban fringe areas. Huang [17] extracted impervious surfaces in the central urban area of Chongqing from 2001 to 2020, studying the spatiotemporal changes and expansion drivers of these surfaces to analyze the urban development process of Chongqing's central urban area. Yin [18] monitored and analyzed the spatiotemporal expansion of impervious surfaces in the Guangdong-Hong Kong–Macao Greater Bay Area from 1990 to 2020 using remote sensing data to reflect the degree of urbanization and urban expansion changes in the study area.

Points of interest (POI) data—easily accessible, open-source big data—can intuitively reflect the spatial distribution characteristics of tangible elements such as urban socio-economic factors and population activity areas [19], thus fully leveraging their advantages in the field of urban spatial structure research. Many scholars have utilized POI data for related studies on urban built-up areas [20,21], urban fringe boundaries [22–24], urban physical areas [25], and urban center determination [26,27]. They have also combined POI data with multiple sources such as urban green space data [28], Weibo check-in data [29], and nighttime light data [30,31] to conduct coupling analyses and explore urban spatial structures. Gao [32] analyzed the spatial structure of Shenzhen by integrating nighttime light data and POI data both spatially and temporally. Chen [33] explored the spatial coupling relationship between nighttime light data and POI kernel density by spatially gridding the data and using dual-factor mapping. Cheng [34] conducted an overlay analysis of nighttime light data and POI data to examine the internal spatial structure of coastal cities. Wang [35] coupled nighttime light data, POI kernel density, and Weibo check-in data to investigate the spatial distribution characteristics of Beijing and analyzed the relationship between spatial distribution and the proportion of the aging population. Yu [36] performed a coupling analysis of nighttime remote sensing data and POI data to examine the relationship between spatially disparate coupling regions and urban spatial structure, using this foundation to discuss the role of ports in the urban structure of Sanya.

In summary, in research on urban spatial structures based on multi-source data, most scholars choose night light data and POI data for coupling analysis, which can also express socioeconomic characteristics. However, night data has inevitable defects. There are often limitations of "oversaturation" and "spillover effect", which reduce the accuracy of the research results [37], and this is reflected in the above research results: compared with the spatial distribution of POI kernel density, the spatial distribution range of nighttime lights is significantly expanded. Impervious surface coverage characterizes the distribution of urban physical buildings, which can effectively avoid this phenomenon. The combination of POI data and impervious surface data can make full use of the advantages of both in different aspects to form a comprehensive description of urban spatial characteristics. POI data can supplement impervious surface data in terms of socio-economic activities and population activities, while impervious surface data can make up for the deficiency of POI data in terms of physical spatial characteristics.

However, current research lacks studies that couple impervious surface data with POI data to explore the correlation between urban built-up areas and human activity density, thereby characterizing urban spatial features. Additionally, the existing studies typically use POI data to analyze density variations, calculating POI kernel density or point density, and often neglect the differences in POI data types. This oversight results in underutilizing the full potential of POI data, significantly reducing the depth and accuracy of urban spatial structure analysis.

Therefore, this paper takes POI data and impervious surface data as the breakthrough point to construct a POI comprehensive index. Starting from the coupling relationship between the POI comprehensive index and impervious surface coverage data that can characterize urban infrastructure, the relationship between the same and different areas of the spatial coupling relationship and urban spatial structures is discussed, and the characteristics of urban internal spatial structures are analyzed. This paper systematically analyzes the characteristics of the same and different regions of the spatial coupling of the POI composite index and impervious surface coverage in the 2022 Beijing–Tianjin–Hebei urban agglomeration. Understanding the coupling pattern of the two types of data allows urban planners to identify areas that need to be prioritized for infrastructure upgrades and economic incentives and promotes a more inclusive urbanization process. It is of great significance to deeply understand the spatial structure law of urban agglomeration and guide the coordinated development of the Beijing–Tianjin–Hebei urban agglomeration.

2. Materials and Methods

2.1. Study Area Overview and Data Sources

2.1.1. Study Area Overview

The spatial extent of the Beijing–Tianjin–Hebei urban agglomeration encompasses two directly administered municipalities, Beijing and Tianjin, along with 11 prefecture-level cities in Hebei Province, covering a total area of 216,000 square kilometers. Situated in the northern part of the North China Plain, the Beijing–Tianjin–Hebei urban agglomeration generally presents a topography characterized by higher elevations in the northwest and lower elevations in the southeast. The study area encompasses Beijing, Tianjin, and the 11 cities within Hebei Province (Figure 1). The total geographical extent of the research region exceeds 210,000 square kilometers, accommodating a permanent population of 113.07 million individuals, and the terrain is varied and intricate. According to statistical yearbook data, farmland constitutes the largest proportion of land use; yet, with ongoing economic development, urban infrastructure has continually expanded, resulting in a gradual rise in the proportion of construction land.

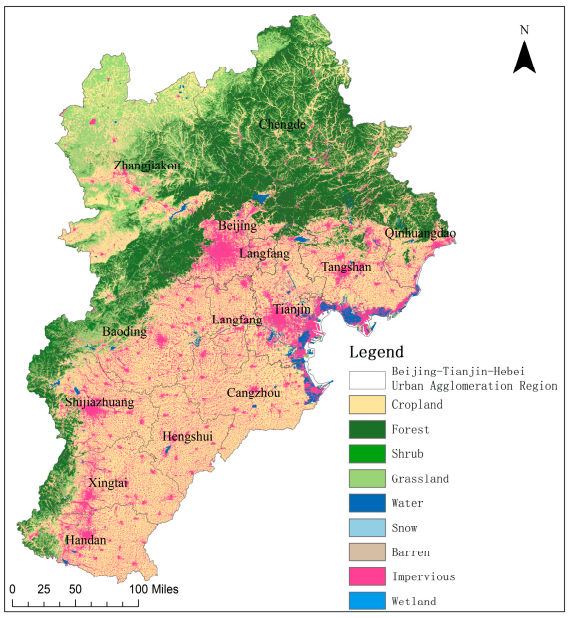

Figure 1. Land use map of Beijing–Tianjin–Hebei.

2.1.2. Data Sources

The research data used in this study are presented in Table 1, including POI data and land use data.

Table 1. Information table of data sources.

Feature	Data	Data Type	Data Source
Basic Geographic Data	MAP	Polygon Vector Data	National Geomatics Center of China (http://www.ngcc.cn/ngcc/, accessed on 5 December 2023)
Social–Economic Data	POI	Point Vector Data	Gaode Map (https://lbs.amap.com/, accessed on 5 February 2024)
Land Use Data	CLCD	Raster Data	The 30 m Annual Land Cover Datasets and their Dynamics in China from 1985 to 2022 [Dataset] (https://doi.org/10.5281/zenodo.8176941, accessed on 5 July 2023)

The POI data utilized in this study were gathered within the Beijing–Tianjin–Hebei urban agglomeration area via the API interface provided by Gaode Map (https://lbs.amap.com/api/webservice/download, accessed on 5 February 2024) Following the acquisition of raw data, preprocessing procedures, including deduplication and filtering, were implemented. The resulting POI dataset comprised over 2.95 million entries, ensuring a comprehensive portrayal of the spatial distribution of resident activities and economic transactions. Gaode Map classifies POI data into three hierarchical levels: primary category, subcategory, and detailed category (Table 2). Since the division of minor classes was too tedious and fine, which was not conducive to subsequent calculation research, this study only carried out the relevant calculation research of primary and subcategories.

Table 2. Summary of POI classification levels in the Beijing–Tianjin–Hebei region.

ID	Major Categories	Subcategories	Quantity	Proportion
01	Transport Facilities	Parking Lots, Bus Stops, etc.	174,859	5.91%
02	Leisure and Sports	KTV, Theaters, etc.	38,051	1.29%
03	Companies and Enterprises	Companies, Factories, etc.	283,411	9.58%
04	Healthcare	Specialized Hospitals, etc.	145,849	4.93%
05	Business Residences	Industrial Parks, etc.	81,551	2.76%
06	Tourist Attractions	Scenic Spots, Parks, etc.	25,235	0.85%
07	Automotive-Related	Charging Stations, etc.	147,017	4.97%
08	Daily Services	Agencies, etc.	368,178	12.45%
09	Education and Culture	Universities, etc.	151,576	5.13%
10	Consumption	Convenience Stores, etc.	909,631	30.76%
11	Sports and Fitness	Gyms, Sports Centers, etc.	38,366	1.30%
12	Hotel Accommodation	Hotels, Motels, etc.	62,020	2.10%
13	Financial Institutions	Insurance, Banks, etc.	51,582	1.74%
14	Catering Industry	Restaurants, Cafes, etc.	480,251	16.24%

2.2. Spatial Coupling Research Methods

The technical pathway of spatial coupling methods is delineated in Figure 2. This pathway primarily encompassed two segments: the construction of indicator data and the visualization of coupling relationships. In the initial segment, indicator data were synthesized through the processing of POI data sourced from the Beijing–Tianjin–Hebei region. A three-dimensional array of POI data was computed, encompassing indices for POI major and subcategories confusion, alongside POI kernel density. Furthermore, a comprehensive POI index was derived utilizing the entropy weight method. Concurrently, land cover data from the Beijing–Tianjin–Hebei region were employed to extract impervious surface type data, facilitating the calculation of an impervious surface coverage index.

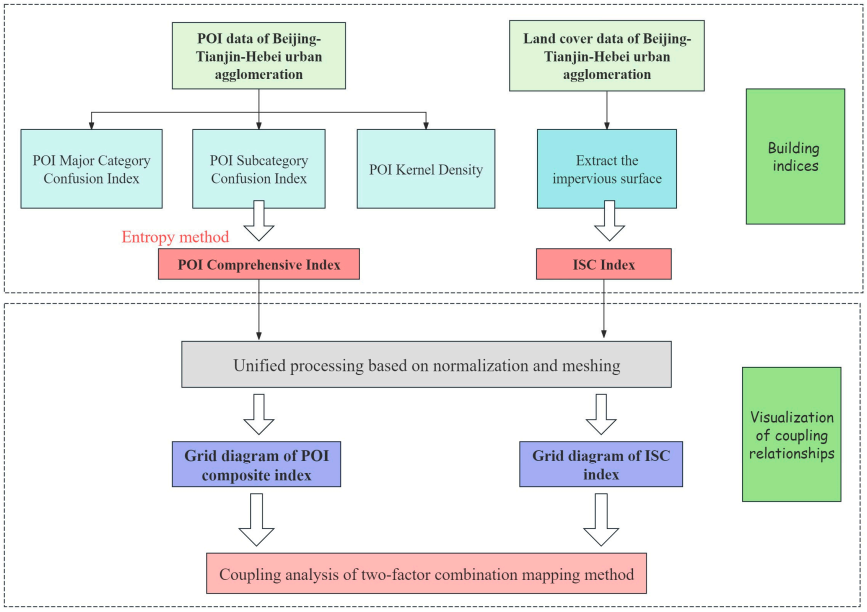

Figure 2. Technical pathway diagram.

In the subsequent segment, the visualization of coupling relationships was facilitated. A grid composed of 1 km × 1 km cells spanning the Beijing–Tianjin–Hebei urban agglomeration was established. The multi-dimensional data were then normalized to a range of [0, 1] using the min–max normalization method, yielding grid maps depicting the POI comprehensive index and impervious surface coverage. Employing a dual-factor mapping approach, visual representations of the spatial coupling relationship between the POI comprehensive index and imperviousness rate were generated. Subsequently, an analysis was conducted to ascertain the degree of spatial coupling between the two datasets. Moreover, the interplay between areas exhibiting similar and dissimilar spatial coupling, alongside the spatial connectivity of the urban agglomeration and the internal spatial structure of cities, was explored based on these visualizations.

2.2.1. Construction of Data Indicators

- POI Confusion Index

A greater diversity of POI types within a grid cell signified a region with more vibrant social activities and economic dynamism. It is an established fact that the diversity and quantity of POI decline gradually from urban cores to rural areas. Exploring urban spatial structures based on this trait is inherently logical. Introducing information entropy into the POI data computation allowed us to discern POI diversity within grid cells.

$$SHDI = -\sum_{n=1}^{N} X_n \ln(X_n) \quad (1)$$

In the formula, X_n represents the proportion of a specific type of POI within the total number of POI in a grid cell and n represents the total number of POI categories in that grid cell unit. In this study, confusion indices for both major and subcategories of POI were computed within grid cells. However, practical computations can experience deviations due to the presence of diverse land parcels where certain types or multiple types of POI are overly abundant. This can lead to significant disparities in the quantities of various POI categories and consequently result in lower confusion indices compared to areas with dominant single-category or balanced quantities. Therefore, alongside calculating confusion indices within grid cells, attention was also paid to the measurement of POI quantities. Calculating POI kernel density helped mitigate this deviation.

- POI Kernel Density

Kernel density serves as a valuable tool for evaluating point distribution density in a geographic space, and particularly for analyzing the distribution of POI across various geographical locations within urban areas. The calculation of POI kernel density relies on the concept of kernel functions, typically computed using the following formula:

$$D(x) = \sum_{i=1}^{n} \frac{K(\frac{\| x - x_i \|}{h})}{h^2} \quad (2)$$

In the equation, $D(x)$ represents the kernel density value at location x, where n is the total number of POI, x_i denotes the coordinates of the ith POI, and $\| x - x_i \|$ represents the distance from point x to point x_i. The bandwidth parameter, denoted by h, determines the range of influence of the kernel function. By adjusting the bandwidth and selecting appropriate kernel functions, varying levels of precision and sensitivity in kernel density estimation can be attained. Following multiple rounds of experimentation and adjustments, a bandwidth of 3000 m was selected in this study to compute the kernel density of the study area. This density was then integrated with confusion indices for major and subcategories of POI to form a comprehensive three-dimensional array of POI within grid cells. This amalgamation of POI kernel density with confusion indices serves as a complementary correction, facilitating a more precise representation of the level of urbanization development in the area.

- Impervious Surface Coverage Index

Impervious surface coverage (ISC) is a continuous variable ranging from 0 to 100%. It represents the proportion of impervious surface land area within a grid cell according to the following formula:

$$ISC = \frac{S_k}{Area_k} \times 100\% \quad (3)$$

In the formula, S_k represents the area of impervious surface within a grid cell and $Area_k$ represents the total area of the grid cell.

A spatial distribution diagram of each index data is shown below (Figure 3).

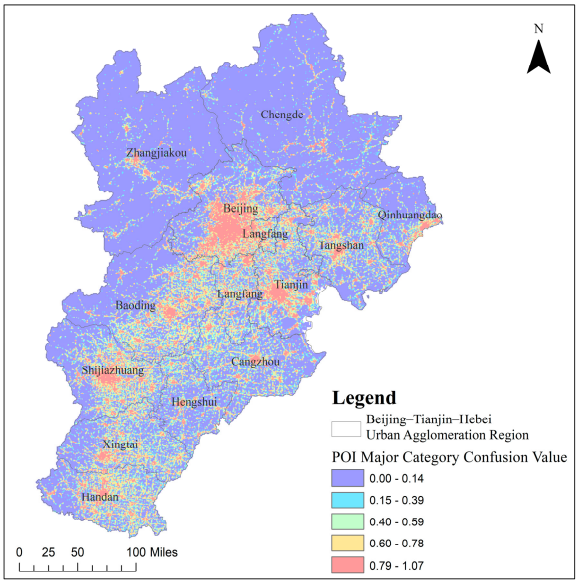

(**a**)

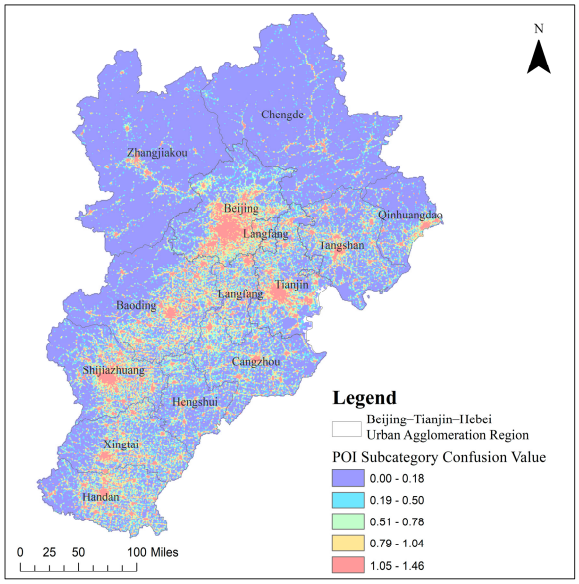

(**b**)

Figure 3. *Cont.*

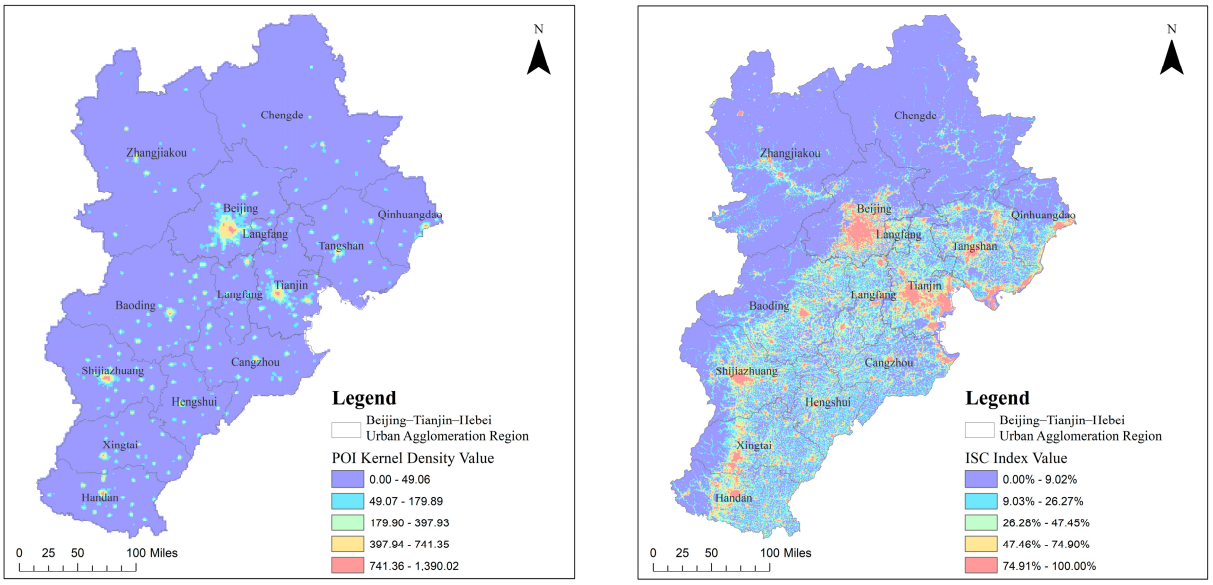

(**c**) (**d**)

Figure 3. Spatial distribution maps of various data types: (**a**) POI major category confusion index, (**b**) POI subcategory confusion index, (**c**) POI kernel density index, (**d**) ISC index.

2.2.2. Construction of POI Comprehensive Indicators

The entropy weight method is a comprehensive evaluation approach that integrates multiple indices, considering their respective weights and contributions to achieve a unified assessment outcome. Rooted in the concept of information entropy, this method computes the entropy and weights associated with each indicator, subsequently conducting a weighted summation of these indicators to yield the ultimate comprehensive evaluation value. The calculation formula is presented as follows.

$$W_i = \frac{1 - E_i}{\sum_{j=1}^{n} (1 - E_i)} \tag{4}$$

$$S_i = \frac{E_i}{\sum_{j=1}^{n} E_i} \tag{5}$$

In the equation, W_i represents the weight of indicator i, E_i denotes the information entropy of indicator i, and S_i represents the score of indicator i. By applying the entropy weight method to comprehensively evaluate the three-dimensional array of POI, we employed POI kernel density and POI confusion indices as assessment metrics. This procedure culminated in the creation of a POI comprehensive index, effectively capturing the comprehensive urbanization level and offering a more nuanced depiction of human activity levels. The spatial distribution map of the POI composite index is shown below (Figure 4).

2.2.3. Two-Factor Combination Mapping

- Data Normalization Process

We used min–max normalization to scale the POI comprehensive index within the range of [0, 1]; the formula is as follows:

$$Y = \frac{X_i - X_{\min}}{X_{\max} - X_{\min}} \tag{6}$$

Y represents the normalized data, X_i represents the original index, and X_{max} and X_{min} represent the maximum and minimum values of the index, respectively.

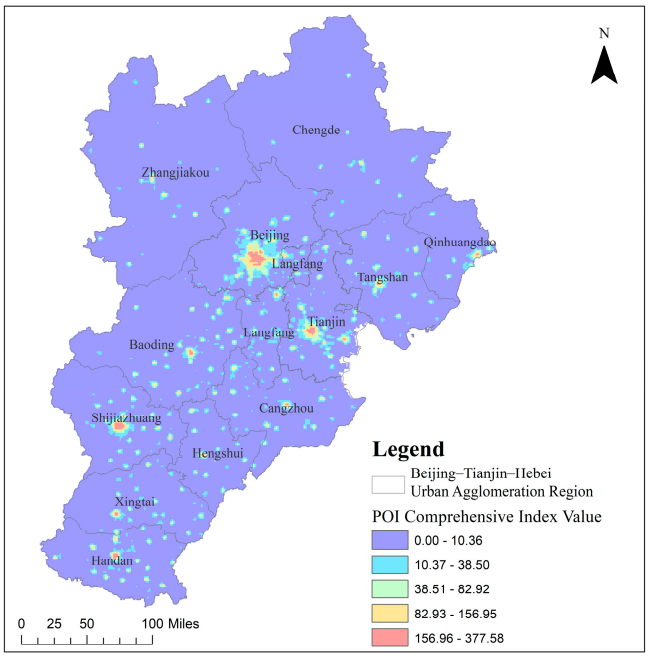

Figure 4. POI comprehensive index of Beijing–Tianjin–Hebei region.

- Principle of Two-Factor Combination Mapping

Two-factor combination mapping is a visualization technique illustrating the interplay between two variables, as exemplified in Figure 5. It yields four combinations based on the magnitudes of the variables, with transitional states between them leading to further variations. To enhance clarity in visual representation, a distinct color scheme was chosen, where gradient transitions delineated the differentiation between combinations. Employing the natural breaks method, the normalized POI comprehensive index and imperviousness rate were stratified into high, medium, and low levels. Spatial connections were then established according to these levels, resulting in nine theoretically possible combination types: high-high, high-medium, high-low, medium-high, medium-medium, medium-low, low-high, low-medium, and low-low.

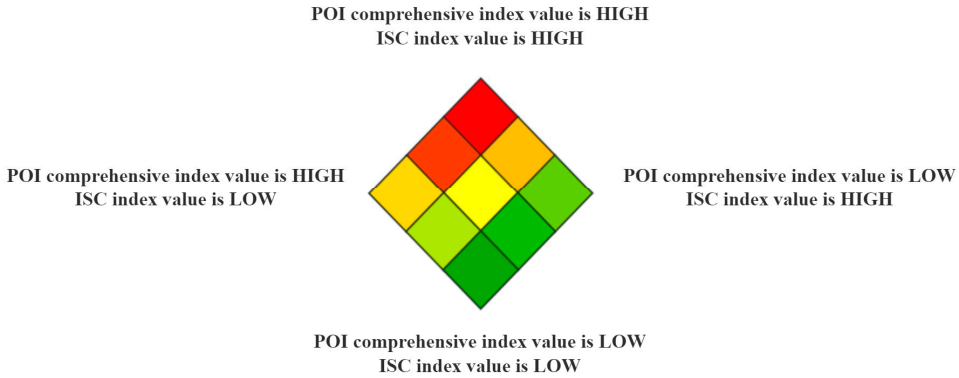

Figure 5. Legend of two-factor combination mapping.

3. Spatial Coupling Analysis Results

3.1. Spatial Coupling Analysis Results

Upon comparing the spatial distribution characteristics of the four indicators (Figure 3), it was evident that the confusion indices for POI subcategories and major categories

displayed significant overlap. However, owing to the finer granularity and diversity within POI subcategories, they offered superior performance in delineating intricate spatial patterns compared to POI major category confusion indices. The distribution of POI confusion indices was marked by fragmented patches and discontinuous, ambiguous zoning. In contrast, POI kernel density showcased a continuous, aggregated distribution pattern with distinct boundaries between high and low values. Nevertheless, high-density areas of POI kernel density were relatively scarce and tended to appear almost point-like. The POI comprehensive index, derived using the entropy weight method, adeptly addressed the shortcomings of both POI kernel density and confusion indices. It exhibited a continuous circular distribution pattern in space while also extending high-value areas with clearly defined boundaries between high and low values. Despite impervious surface coverage also exhibiting fragmented patches in its spatial distribution, the delineation between high and low values remained clear. In essence, there existed consistency in the spatial distribution trends across the various data types.

The comprehensive indices of POI and impervious surface coverage data within the Beijing–Tianjin–Hebei region exhibited analogous spatial distribution patterns across most urban areas, showing a prevalent expansion trend from the central districts of Beijing toward the east and south. Predominantly, contiguous patches of high-value areas were concentrated in the central zones of Beijing, Tianjin, and Shijiazhuang, with smaller yet coherent high-value regions also observed in Handan and Xingtai. Moreover, suburban regions surrounding each city showcased scattered or patchy high-value areas in both the POI comprehensive index and impervious surface coverage. Notably, Zhangjiakou and Chengde, situated within the northwest ecological conservation area outlined in the coordinated development plan for Beijing–Tianjin–Hebei, featured extensive mountainous terrain, resulting in relatively fewer high-value areas in the spatial distribution of both the POI comprehensive index and impervious surface coverage. The spatial distribution of the POI composite index and impervious surface coverage revealed their indicative effects on the urbanization process. Areas with dense POI and high impervious surface coverage usually showed advanced urbanized areas, such as Beijing and Tianjin. These regions have excellent infrastructure, extensive public services, and a vibrant economic environment. The diverse POIs in these areas attract population inflows and further accelerate urban growth and development.

Figure 6 shows that in the coupled spatial distribution of the POI comprehensive index and impervious surface cover in the Beijing–Tianjin–Hebei region, urbanization and human activities in the Beijing–Tianjin–Hebei region are highly concentrated in specific areas, while most other areas maintain a low degree of development. Coupled regions shared by the Beijing–Tianjin–Hebei urban agglomeration represent 69.19% of the entire urban area. The high coupling of POI indices and impervious surface coverage was prominent in highly urbanized areas, notably in administrative hubs such as Beijing, Tianjin, and Shijiazhuang, which are economically developed regions within the urban agglomeration. Widespread low-low coupling suggested numerous areas with lower human activity density and fewer impervious surfaces, indicating relatively incomplete urban infrastructure. Mid-mid coupling areas were sparsely distributed, mainly around the periphery of urban centers, aligning with the developmental pattern of urban structures expanding outward from the center. High-high and mid-mid coupling areas generally corresponded to economically developed regions with higher GDP rankings within the regional hierarchy. These identified areas also provided insights into the locations of built-up areas within administrative regions. In areas with more advanced urban land development, low-low coupling areas typically encompassed bodies of water and mountainous regions not commercially developed for ecological conservation purposes. These areas exhibited significant characteristics of very low POI comprehensive indices and impervious surface coverage.

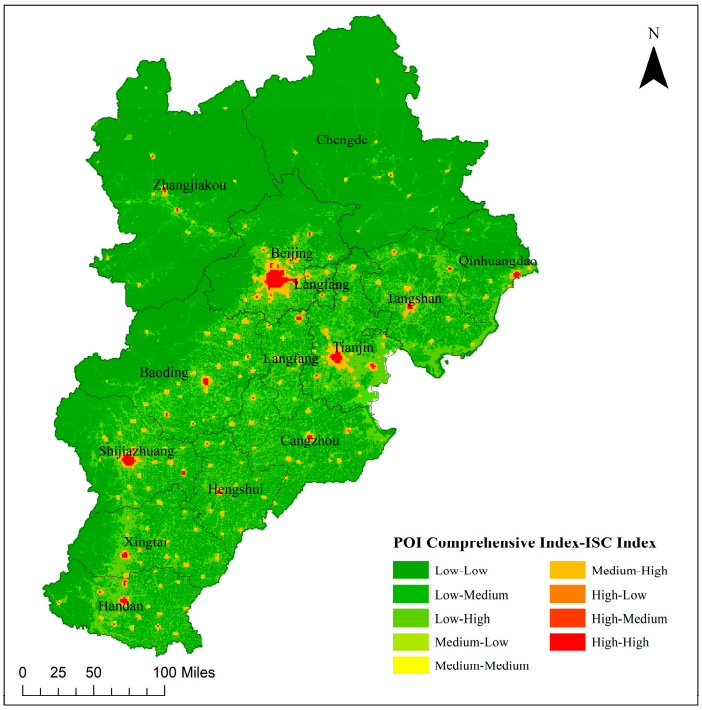

Figure 6. Spatial coupling relationship between the comprehensive POI index and ISC in the Beijing–Tianjin–Hebei region.

An analysis of coupling levels between the comprehensive POI index and impervious surface coverage in the Beijing–Tianjin–Hebei urban agglomeration revealed distinct patterns: areas where the POI comprehensive index was lower than the impervious surface coverage covered 40.73% of the total area, while those where the POI comprehensive index exceeded the impervious surface coverage constituted only 0.07% of the total area. Combining remote sensing images enhanced our understanding of the relationship between urban development and population density across areas with varying coupling levels. Figure 7 showcases satellite imagery of regions with diverse coupling levels at a resolution of 1km*1km, highlighting spatial heterogeneity among these regions. High-high coupling areas displayed pronounced urban features, mainly situated in urban cores characterized by dense clusters of buildings and consistent land cover types. Mid-high coupling areas served as transition zones between urban cores and rural peripheries, marked by reduced building density and greater land cover diversity. Low-medium coupling areas typically represented rural landscapes, where remote sensing imagery revealed the distribution of villages and farmland. Such regions exhibited sparse POI distribution and limited variety, resulting in a lower POI comprehensive index. Low-low coupling areas primarily comprised remote terrains like mountains and bodies of water with minimal infrastructure, sparse populations, low human activity density, and limited construction activity.



(**a**) (**b**) (**c**) (**d**)

Figure 7. Spatial distribution maps of various data types: (**a**) high-high, (**b**) medium-high, (**c**) medium-low, (**d**) low-low.

3.2. Analysis of Typical Urban Coupling Relationships

3.2.1. Analysis of Spatial Structures in Cities with Similar Coupling

In this study, Beijing, Tianjin, and Shijiazhuang were selected as typical cities to analyze the coupling results, and the spatial distribution map of the calculation results is shown below (Figure 8). The prevalence of areas exhibiting identical coupling between the POI comprehensive index and impervious surface coverage was noteworthy. These regions served as indicators of the developmental stage of urban infrastructure. High-high coupling areas denoted highly urbanized regions, distinguished by well-established infrastructure and a diverse array of social activities among residents. In contrast, mid-mid coupling areas constituted a minority of the distribution, often displaying scattered patterns around central urban zones. These areas represented transitional zones undergoing the process of urbanization, bridging the gap between urban and rural landscapes. Covering the largest area, low-low coupling areas were characterized by minimal or absent infrastructure, with sparse human habitation or activity. These regions were predominantly situated in remote mountainous or forested terrain or rural areas distant from urban centers.

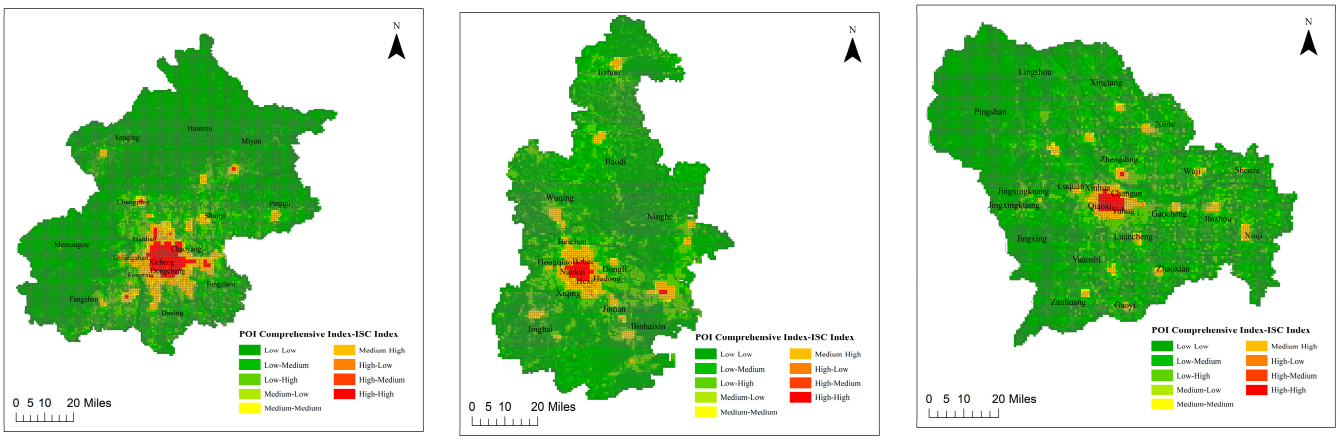

(**a**) (**b**) (**c**)

Figure 8. Distribution map of spatial coupling relationship between POI comprehensive index and ISC: (**a**) Beijing, (**b**) Tianjin, (**c**) Shijiazhuang.

In Beijing, regions with identical coupling represented 73.39% of the total area. As depicted in Figure 9, low-low coupling areas were notably prevalent, primarily concentrated in the mountainous terrain of western and northern Beijing. Conversely, mid-mid coupling areas constituted the smallest fraction, scattered irregularly along the city's periphery. High-high coupling zones were predominantly situated in the densely urbanized central regions encompassing Beijing's six core districts, including Dongcheng and Xicheng entirely, the western expanse of Chaoyang District, the southeastern sector of Haidian District, and the eastern precinct of Fengtai District.

In Tianjin, regions displaying identical coupling represented 64.37% of the total area. Among these, low-low coupling areas occupied the largest share, while contiguous high-high coupling zones were concentrated within the Nankai, Hexi, Hebei, and Hedong Districts. Furthermore, central areas within Wuqing, Baodi, Jinghai, and Binhai New Area manifested notable instances of high-value coupling.

In Shijiazhuang, areas with identical coupling covered 63.78% of the total area, echoing the patterns observed in Beijing and Tianjin. Low-low coupling areas exhibited the most extensive distribution, while high-high coupling zones prominently appeared in the central regions of the Xinhua, Chang'an, Qiaoxi, and Yuhua Districts. Mid-mid coupling areas were sporadically scattered along the urban periphery.

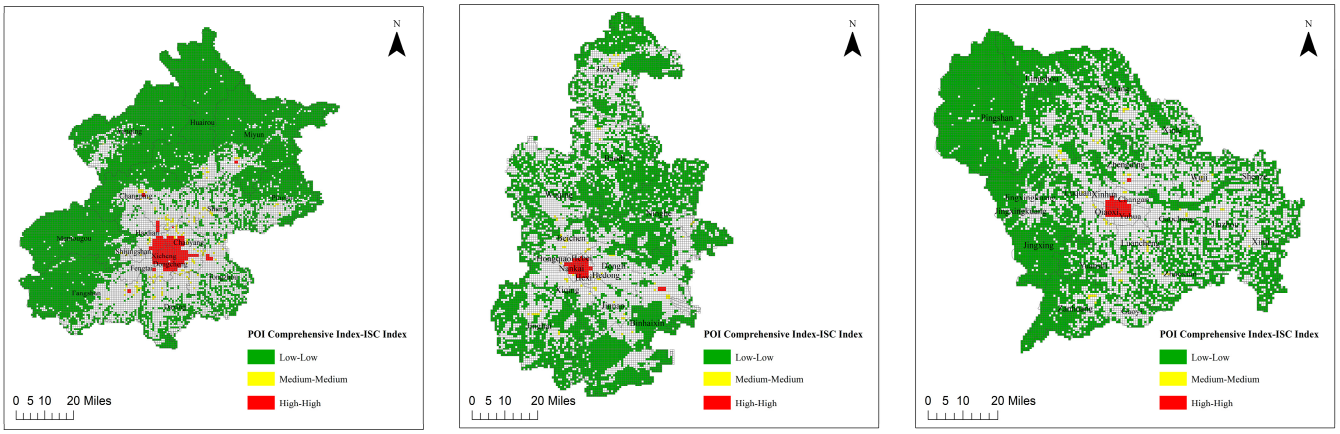

(a) (b) (c)

Figure 9. Regional distribution of POI comprehensive index and ISC equivalence: (**a**) Beijing, (**b**) Tianjin, (**c**) Shijiazhuang.

3.2.2. Analysis of Spatial Structures in Cities with Different Coupling

1. Areas where the POI comprehensive index was lower than the impervious surface coverage

In the spatial distribution of the coupling relationship between the POI comprehensive index and impervious surface coverage, certain regions exhibited an incomplete coupling state, which held significant implications for urban structural studies. Areas where impervious surface coverage surpassed the POI comprehensive index, depicted in Figure 10, demonstrated similar distribution trends across Beijing, Tianjin, and Shijiazhuang. The continuous circular coupling relationship between mid and high regions of the POI comprehensive index and impervious surface coverage was primarily situated on the periphery of core urban areas, with sporadic occurrences in various districts representing district centers. This coupling pattern indicated relatively well-established infrastructure and lower population activity density compared to the core urban areas, suggesting lower urban development intensity overall. Conversely, areas where the POI comprehensive index fell below the impervious surface coverage were predominantly distributed surrounding the mid-to-high regions, serving as transition zones from suburban areas or villages to urban or town centers. Conversely, regions with low-to-mid coupling disparities demonstrated relatively underdeveloped and incomplete infrastructure. The majority of POI data in these areas were associated with industrial or service industries, exhibiting lower quantities and varieties, primarily concentrated in suburban and rural regions.

Furthermore, areas hosting well-established facilities such as airports, ports, and train stations often demonstrated high impervious surface coverage owing to their comprehensive infrastructure. Nevertheless, these regions typically exhibited relatively lower levels of human activity and a restricted diversity of POI, despite their widespread presence, which tended to serve singular functions. Consequently, scenarios emerged where impervious surface coverage registered high values, while the POI comprehensive index remained comparatively low. This phenomenon was commonly observed in areas characterized by disparities in coupling, particularly in instances of low-to-high coupling. For instance, locales such as the vicinity of Beijing Capital International Airport in Shunyi District, Beijing Miyun Mujiayu Airport in Miyun District, Tongzhou West Railway Station in Tongzhou District, Shijiazhuang Zhengding International Airport, and ports in the Binhai New Area of Tianjin exemplified regions where the POI comprehensive index exhibited low-to-high coupling with impervious surface coverage.

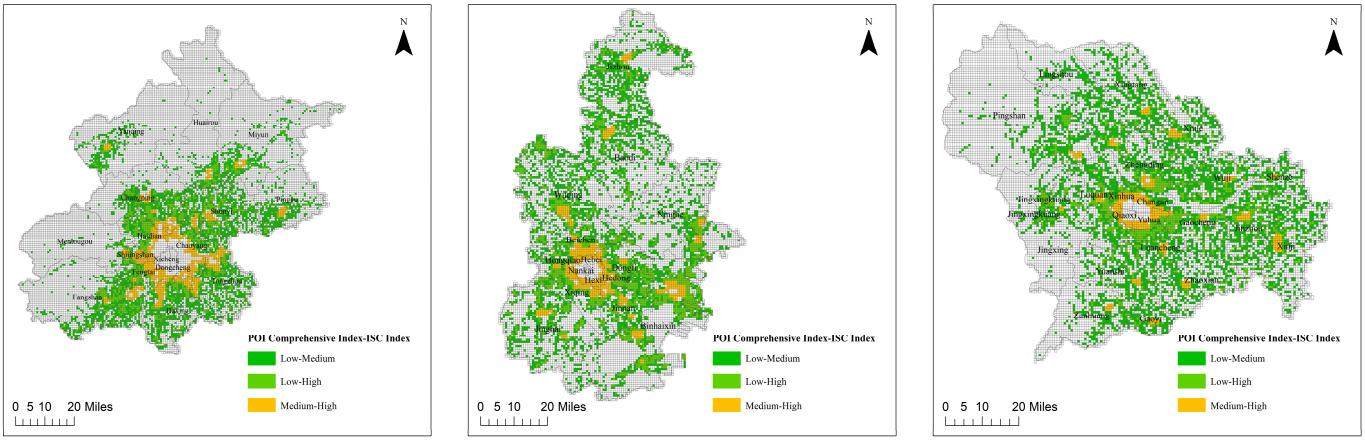

(**a**) (**b**) (**c**)

Figure 10. Regional distribution map showing where POI comprehensive index values were lower than ISC values: (**a**) Beijing, (**b**) Tianjin, (**c**) Shijiazhuang.

2. Areas where the POI comprehensive index was higher than the impervious surface coverage

The areas where the POI comprehensive index exceeded impervious surface coverage are depicted in Figure 11. It is apparent from the figure that there were few instances where the POI comprehensive index was higher than impervious surface coverage, appearing as scattered points.

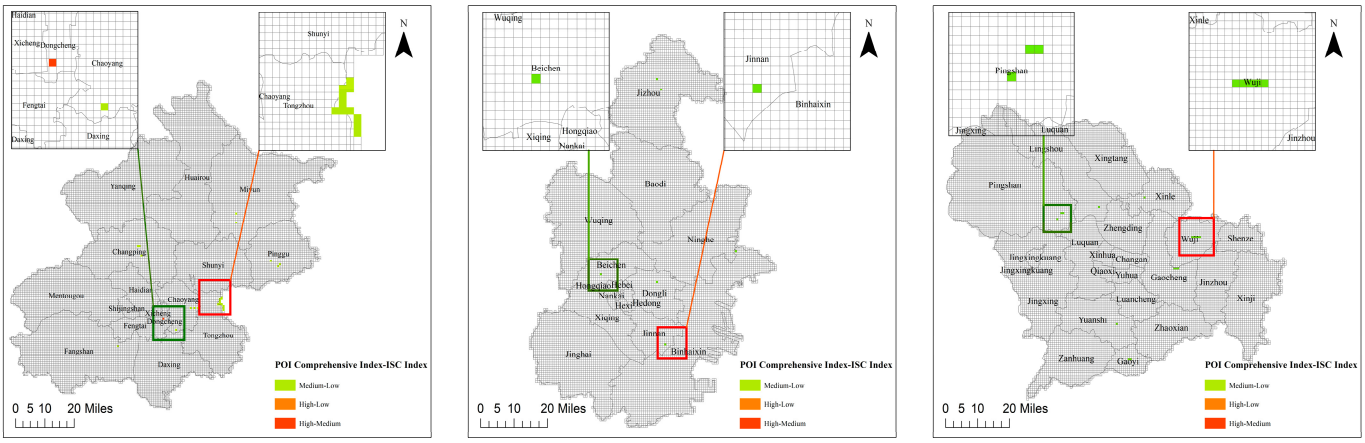

(**a**) (**b**) (**c**)

Figure 11. Regional distribution map showing where POI comprehensive index values were higher than ISC values: (**a**) Beijing, (**b**) Tianjin, (**c**) Shijiazhuang.

In Beijing, Dongcheng District demonstrated high-to-mid coupling, with coordinates indicating the Temple of Heaven Park's location. This park, a renowned scenic spot in Beijing, boasted a plethora of nearby POIs. Moreover, owing to the extensive greenery within the Temple of Heaven Park, the POI comprehensive index in this area surpassed the impervious surface coverage. Mid-to-low coupling regions were dispersed across Changping District, Miyun District, Pinggu District, Chaoyang District, Fangshan District, and Tongzhou District. In the eastern part of Tongzhou District, the mid-to-low coupling area encompassed Xiaoyang Park, Chaobai River Park, Chaobai River Yanjiao Park, and the Beijing Tongzhou Canal Garden Resort, all clustered along the Grand Canal. Similarly, in the eastern part of Chaoyang District, the mid-to-low coupling area included the Changying Marathon Sports Park. The mid-to-low coupling areas in Pinggu District, Fangshan District,

Miyun District, and Changping District stemmed from the partitioning of large swathes of mountains, forests, or farmland, alongside small pockets of villages within the same grid cell during the partitioning process, resulting in diminished impervious surface coverage within those cells.

Tianjin and Shijiazhuang, areas where the POI comprehensive index was higher than the impervious surface coverage, exhibited predominantly mid-to-low coupling relationships, primarily located in the outskirts of specific districts. Upon integrating remote sensing imagery, it was noted that these areas of coupling disparity largely consisted of parks, scenic spots, and other residential activity zones. These regions shared common land cover characteristics such as farmland, forests, or bodies of water, resulting in low impervious surface coverage. Consequently, situations arose where the POI comprehensive index surpassed the impervious surface coverage.

4. Conclusions

This study conducted an analysis of the spatial coupling relationship between the comprehensive POI index and impervious surface coverage in the Beijing–Tianjin–Hebei region in 2022, investigating the spatial characteristics of both the POI comprehensive index and impervious surface coverage. The main conclusions are derived from the exploration of the spatial distribution of the disparate regions between them and their relationship with urban spatial structures:

(1) The relationship between the comprehensive POI index and impervious surface coverage was consistent and aligned well, as demonstrated by the use of information entropy and entropy weight methods. Across the Beijing–Tianjin–Hebei urban agglomeration, the overall spatial distribution patterns of both datasets remained consistent, with regions demonstrating identical spatial coupling relationships accounting for 69.19% of the total area. Specifically, in Beijing, these regions represented 73.39% of the total area, while in Tianjin and Shijiazhuang, they represented 64.37% and 63.78%, respectively. This effectively delineated the spatial morphology of urban cores and surrounding towns in each city, thereby confirming the utility of the comprehensive POI index in analyzing urban spatial structures.

(2) The regions where the comprehensive POI index was lower than impervious surface coverage, displaying spatial disparities, could effectively delineate the spatial characteristics of specific urban structures, such as expansive homogeneous zones, urban peripheries, suburban areas, and town centers and their respective levels of urbanization. There were discernible disparities in the spatial attributes of the two datasets: POI data exhibited a relatively sparse distribution in economic development zones, emerging urban areas, airports, ports, etc., but demonstrated a certain degree of presence in suburban areas and town centers. Conversely, impervious surface coverage demonstrated heightened intensity in urban core areas, economic development zones, airports, ports, and other regions boasting well-established infrastructure.

(3) The spatially distinct areas where the comprehensive POI index surpassed impervious surface coverage were less common within urban structures, consistent with the pattern where infrastructure development precedes economic progress in urban areas. These zones were typically found in areas characterized by larger expanses of green space, farmland, bodies of water, parks, mountains, and scenic areas.

This paper studied the qualitative coupling analysis of land use and POI data in 2022 and discussed the spatial structure of the Beijing–Tianjin–Hebei urban agglomeration. By using the coupling degree of the POI comprehensive index and impervious surface cover data, urban planners can more accurately identify urban centers, marginal areas, and rural areas. This facilitates more targeted land-use planning and infrastructure investment, avoiding resource wastage and overdevelopment. Understanding the coupled patterns of both types of data simultaneously allows urban planners to identify priority areas for infrastructure upgrades and economic incentives, promoting a more inclusive urbanization process. It is of great significance to deeply understand the spatial structure law of urban

agglomeration and guide the coordinated development of the Beijing–Tianjin–Hebei urban agglomeration. In future studies, multi-time and multi-source data can be added to integrate spatial coupling and conduct comparative studies on spatial and temporal scales. In addition, POI and other multi-source data can be classified and coupled to further analyze the urban spatial structure by classification, provide a new perspective for the spatial structure research of the Beijing–Tianjin–Hebei urban agglomeration, deeply understand the spatial structure law of urban agglomeration, and guide the coordinated development of the Beijing–Tianjin–Hebei urban agglomeration.

Author Contributions: Conceptualization, T.Z. and X.Z.; Data curation, T.Z.; Formal analysis, Y.L., C.J. and H.B.; Investigation, T.Z. and C.J.; Methodology, X.Z. and H.B.; Project administration, X.Z.; Resources, T.Z.; Validation, T.Z., X.Z. and Y.L.; Visualization, T.Z. and H.B.; Writing—original draft, T.Z. and X.Z.; Writing—review and editing, T.Z., X.Z., Y.L. and C.J. All authors have read and agreed to the published version of the manuscript.

Funding: Hebei Provincial Department of Education, ZD2022041.

Data Availability Statement: Data are available within the paper or upon reasonable request.

Conflicts of Interest: The authors declare no conflicts of interest.

References

1. Elmqvist, T.; Andersson, E.; McPhearson, T.; Bai, X.; Bettencourt, L.; Brondizio, E.; Colding, J.; Daily, G.; Folke, C.; Grimm, N.; et al. Urbanization in and for the Anthropocene. *NPJ Urban Sustain.* **2021**, *1*, 6. [CrossRef]
2. Qu, Y.; Zhan, L.; Jiang, G.; Ma, W.; Dong, X. How to Address "Population Decline and Land Expansion (PDLE)" of rural residential areas in the process of Urbanization:A comparative regional analysis of human-land interaction in Shandong Province. *Habitat Int.* **2021**, *117*, 102441. [CrossRef]
3. Liu, X.; Li, X.; Yang, J.; Fan, H.; Zhang, J.; Zhang, Y. How to resolve the conflicts of urban functional space in planning: A perspective of urban moderate boundary. *Ecol. Indic.* **2022**, *144*, 109495. [CrossRef]
4. Hu, Q.; Shen, W.; Zhang, Z. How does urbanisation affect the evolution of territorial space composite function? *Appl. Geogr.* **2023**, *155*, 102976. [CrossRef]
5. Yanbo, Q.; Shilei, W.; Yaya, T.; Guanghui, J.; Tao, Z.; Liang, M. Territorial spatial planning for regional high-quality development–An analytical framework for the identification, mediation and transmission of potential land utilization conflicts in the Yellow River Delta. *Land Use Policy* **2023**, *125*, 106462. [CrossRef]
6. Zhou, L.; Wei, L.; López-Carr, D.; Dang, X.; Yuan, B.; Yuan, Z. Identification of irregular extension features and fragmented spatial governance within urban fringe areas. *Appl. Geogr.* **2024**, *162*, 103172. [CrossRef]
7. Liu, X.; Li, X.; Zhang, Y.; Wang, Y.; Chen, J.; Geng, Y. Spatiotemporal evolution and relationship between construction land expansion and territorial space conflicts at the county level in Jiangsu Province. *Ecol. Indic.* **2023**, *154*, 110662. [CrossRef]
8. Xiao, R.; Yu, X.; Xiang, T.; Zhang, Z.; Wang, X.; Wu, J. Exploring the coordination between physical space expansion and social space growth of China's urban agglomerations based on hierarchical analysis. *Land Use Policy* **2021**, *109*, 105700. [CrossRef]
9. Lu, B. Urbanization, Spatial Planning and Reproduction of Urban-Rural Relationship: A Case Study of a Suburban Village in China. *Chin. J. Sociol.* **2024**, *44*, 98–124. [CrossRef]
10. Zheng, J.F.; Chen, Q.H. Monocentricity or Polycentricity: On Urban Internal Spatial Structure of Chinese Cities. *China Econ. Stud.* **2019**, *2*, 93–105. [CrossRef]
11. Liu, X.; Li, Y.; Zhang, S.; Niu, Q. Spatiotemporal patterns, driving mechanism, and multi-scenario simulation of urban expansion in Min Delta Region, China. *Ecol. Indic.* **2024**, *158*, 111312. [CrossRef]
12. Wang, H.; Gong, X.; Wang, B.; Deng, C.; Cao, Q. Urban development analysis using built-up area maps based on multiple high-resolution satellite data. *Int. J. Appl. Earth Obs. Geoinf.* **2021**, *103*, 102500. [CrossRef]
13. Peng, J.; Zhao, S.; Liu, Y.; Tian, L. Identifying the urban-rural fringe using wavelet transform and kernel density estimation: A case study in Beijing City, China. *Environ. Model. Softw.* **2016**, *83*, 286–302. [CrossRef]
14. Liang, J.Z.; Xu, Z. Spatial Division in Yangtze River Delta Urban Agglomerations and Expansion Feature Analysis of Rural-Urban Fringe Area. *J. Huaqiao Univ. (Nat. Sci.)* **2022**, *4301*, 102–110. [CrossRef]
15. Ding, X.; Shao, X.; Deng, R.; Peng, S.; Wang, J. Spatiotemporal Dynamics and Driving Forces of Impervious Surfaces in the Central Yunnan Urban Agglomeration from 2000 to 2020. *Res. Soil Water Conserv.* **2024**, *31*, 364–373. [CrossRef]
16. Zhou, X.C.; Liu, Y.M.; Yang, H.J. Spatial recognition and boundary region division of urban fringe area in Xi'an City. *J. Geo-Inf. Sci.* **2017**, *19*, 1327–1335. [CrossRef]
17. Huang, L.; Gu, D.; Liu, Y. Spatiotemporal Evolution of Impervious Surface and the Driving Factors in the Central Urban Area of Chongqing. *J. Southwest Univ.* **2023**, *45*, 155–165. [CrossRef]
18. Yin, Z.; Zhou, T.; Li, H.; Xie, S.; Ren, Y. Study on Impervious Surface Change and Urban Expansion of the Guangdong-Hong Kong-Macao Greater Bay Area. *Geogr. Geo-Inf. Sci.* **2021**, *37*, 106–113.

19. Zhao, H.B.; Yu, D.F.; Miao, C.H.; Li, G.; Feng, Y.; Bie, Q. The Location Distribution Characteristics and Influencing Factors of Cultural Facilities in Zhengzhou Based on POI Data. *Sci. Geogr. Sin.* **2018**, *38*, 1525–1534.
20. Xu, Z.; Gao, X. A novel method for identifying the boundary of urban built-up. *Acta Ecol. Sin.* **2016**, *71*, 928–939. [CrossRef]
21. Tang, C.; Chen, J.; Xie, Y.; Tang, J.; Zhou, C. Integrated Identification and Spatial Differentiation Mechanism of Urban Built-up Area in Changsha-Zhuzhou-Xiangtan Urban Agglomeration Based on the Multi-source Big Data. *Econ. Geogr.* **2024**, *44*, 66–76. [CrossRef]
22. Long, Y.; Luo, S.; Liu, X.; Luo, T.; Liu, X. Research on the Dynamic Evolution of the Landscape Pattern in the Urban Fringe Area of Wuhan from 2000 to 2020. *ISPRS Int. J. Geo-Inf.* **2022**, *11*, 483. [CrossRef]
23. Wang, W.; Gu, Y.; Zhang, C.; Kang, Q.; Yin, W.; Xin, J.; Liao, X. Study on the distribution of urban-rural ecotone in Xianfeng County based on POI and kernel density analysis. *Resour. Environ. Eng.* **2022**, *36*, 117–123. [CrossRef]
24. Sun, X.; Liu, X.; Zhou, Y. Delineating Peri-Urban Areas Using Multi-Source Geo-Data: A Neural Network Approach and SHAP Explanation. *Remote Sens.* **2023**, *15*, 4106. [CrossRef]
25. Zhan, W.; Ban, P.; Yuan, Q. Guangzhou-Foshan Cross-boundary City Zoning Based on Multi-source Data. *South Archit.* **2022**, 10–17. [CrossRef]
26. Duan, Y.M.; Liu, Y.; Liu, X.H.; Wang, H.L. Identification of Polycentric Urban Structure of Central Chongqing Using Points of Interest Big Data. *J. Nat. Resour.* **2018**, *33*, 788–800. [CrossRef]
27. Jiang, Y.Q.; Zhao, X.Z.; Li, P.Q.; Xiang, L.; Zhang, D.K. Quantitative identification method of urban multi-center based on multi-source open data. *J. Geo-Inf. Sci.* **2024**, *26*, 1212–1228. [CrossRef]
28. Dong, R.C.; Jiang, T.Q.; Li, H.H.; Li, S.Y.; Zhang, Y.L.; Fu, X. Service radii analysis of green space based on electronic navigation map POI in Beijing urban area. *Acta Ecol. Sin.* **2018**, *38*, 8536–8543. [CrossRef]
29. Zhang, X.; Sun, Y.; Zheng, A.; Wang, Y. A New Approach to Refining Land Use Types: Predicting Point-of-Interest Categories Using Weibo Check-in Data. *ISPRS Int. J. Geo-Inf.* **2020**, *9*, 124. [CrossRef]
30. Wu, Z.; Wei, X.; He, X.; Gao, W. Identifying Urban Built-Up Areas Based on Spatial Coupling between Nighttime Light Data and POI: A Case Study of Changchun. *Buildings* **2023**, *14*, 19. [CrossRef]
31. Zhang, J.; Yuan, X.-D.; Lin, H. The Extraction of Urban Built-up Areas by Integrating Night-time Light and POI Data—A Case Study of Kunming, China. *IEEE Access* **2021**, *9*, 22417–22429.
32. Gao, Y.; Xing, H.; Zhang, H. Urban spatial structure based on spatial coupling between nighttime light data and POI: A case study of Shenzhen. *J. Guilin Univ. Technol.* **2022**, *42*, 122–130. [CrossRef]
33. Chen, B.; Xu, S.Z.; Zhang, Y.Y.; Xu, F.L.; Wang, H.Z. Analysis of urban spatial structure based on spatial coupling between POI and nighttime data: A case study of main urban region in Wuhan. *Bull. Surv. Mapp.* **2020**, *7*, 70–75.
34. Cheng, S.; Yang, L.; Sun, A. Analysis of urban spatial structure under coupling relationship between night-light data and POI. *Mod. Bus. Trade Ind.* **2022**, *43*, 235–237. [CrossRef]
35. Wang, Y.; Wang, Z.; Deng, Z.; Cheng, P.; Li, Y. Spatial Coupling Analysis Between POI, Luminous Remote Sensing and Weibo Sign-in Data: A Case Study of Beijing. *Remote Sens. Inf.* **2019**, *34*, 18–26. [CrossRef]
36. Yu, B.C.; Liu, Y.X.; Chen, G. Urban spatial structure of port city in South China Sea based on spatial coupling between nighttime light data and POI. *J. Geo-Inf. Sci.* **2018**, *20*, 854–861. [CrossRef]
37. Yuan, X.; Chen, B.; He, X.; Zhang, G.; Zhou, C. Spatial Differentiation and Influencing Factors of Tertiary Industry in the Pearl River Delta Urban Agglomeration. *Land* **2024**, *13*, 172. [CrossRef]

Disclaimer/Publisher's Note: The statements, opinions and data contained in all publications are solely those of the individual author(s) and contributor(s) and not of MDPI and/or the editor(s). MDPI and/or the editor(s) disclaim responsibility for any injury to people or property resulting from any ideas, methods, instructions or products referred to in the content.